Available online at www.sciencedirect.com
SCIENCE DIRECT®
Journal of Organometallic Chemistry 691 (2006) 97–104
Journal of Organometallic Chemistry
www.elsevier.com/locate/jorganchem

Triosmium clusters containing bridging dppm and EPh (E = S, Te) ligands: X-ray structures of $[(\mu\text{-H})Os_3(CO)_7(\mu\text{-SPh})\{\mu_3\text{-}\eta^4\text{-}Ph_2PCHP(Ph)C_6H_4\}]$, $[Os_3(CO)_8(\mu\text{-SPh})_2(\mu\text{-dppm})]$ and $[Os_3(CO)_8(\mu\text{-TePh})_2(\mu\text{-dppm})]$

Shariff E. Kabir [a,*], Madhu S. Saha [a], Derek A. Tocher [*,b], G.M. Golzar Hossain [c], Edward Rosenberg [*,d]

[a] Department of Chemistry, Jahangirnagar University, Savar, Dhaka 1342, Bangladesh
[b] Department of Chemistry, University College London, 20 Gordon Street, London WC1H 0AJ, UK
[c] Department of Chemistry, Cardiff University, P.O. Box 912, Cardiff CF10 3TB, UK
[d] Department of Chemistry, The University of Montana, Missoula, MT 59812, USA

Received 14 July 2005; received in revised form 26 August 2005; accepted 26 August 2005
Available online 11 October 2005

Abstract

Heating $[Os_3(CO)_{10}(\mu\text{-dppm})]$ (**1**) with two equivalents of PhSSPh in toluene under reflux provided three new triosmium compounds $[(\mu\text{-H})Os_3(CO)_7(\mu\text{-SPh})\{\mu_3\text{-}\eta^4\text{-}Ph_2PCHP(Ph)C_6H_4\}]$ (**2**), $[Os_3(CO)_8(\mu\text{-SPh})_2(\mu\text{-dppm})]$ (**3**) and $[(\mu\text{-H})Os_3(CO)_7(\mu\text{-}\eta^2\text{-}SC_6H_4)(\mu\text{-SPh})(\mu\text{-dppm})]$ (**4**) in 20%, 21% and 26% yields, respectively. In contrast, a similar reaction of **1** with two equivalents of PhTeTePh in refluxing toluene gave the binuclear compound $[Os_2(CO)_4(\mu\text{-TePh})_2(\mu\text{-dppm})]$ (**6**) in 15% yield, and two 50 electron isomeric compounds **5** and **7** with the formula $[Os_3(CO)_8(\mu\text{-TePh})_2(\mu\text{-dppm})]$ in 20% and 23% yields, respectively. Thermolysis of **3** at 110 °C afforded **4** in 53% yield which on further thermolysis in refluxing octane at 128 °C gave **2** in 45% yield. Thermolysis of **3** in refluxing octane also gave **2** in 50% yield. The new compounds, **2–7**, were all spectroscopically characterized, and the X-ray structures of **2**, **3** and **7** have been determined. Compound **2** contains a bridging SPh ligand and a $\mu_3,\eta^4\text{-}Ph_2PCHP(Ph)C_6H_4$ ligand, formed by two kinds of C–H activation, including orthometallation of a phenyl group as well as an unusual activation of the methylene group of the dppm ligand. The molecular structure of **3** reveals that two SPh groups span the open Os–Os edge of the Os_3 triangle, while the dppm ligand bridges one of the closed Os–Os edges. In compound **7**, one TePh group spans the open Os–Os edge, while the other spans one of the two closed Os–Os edges and the dppm ligand bridges the third Os–Os vector.

Keywords: Triosmium carbonyl clusters; Diphenyldisulfide; Diphenylditelluride; Bis(diphenylphosphino)methane; X-ray structures

1. Introduction

Transition metal carbonyl compounds containing chalcogen atoms have attracted much attention in recent years owing to their importance in fundamental research as well as in technological fields [1–3]. The presence of chalcogenide atoms appears to often be decisive in cluster aggregation and condensation reactions [4–10]. The main entry into chalcogenido carbonyl species is by the facile oxidative addition of $Ph_3P{=}E$ (E = S, Se, Te) to zero-valent metal centers which commonly generates tertiary phosphine substituted clusters with capping chalcogenide elements [11]. Another approach to the synthesis of bridging chalcogenide metal carbonyl clusters is the cleavage of E–E bonds of diphenyldichalcogenide ligands [12]. For example, Lewis et al. [13] and Arce et al. [14] reported that the reaction of

* Corresponding author. Tel.: +1 406 243 2592; fax: +1 406 243 2477.
E-mail addresses: skabir_ju@yahoo.com (S.E. Kabir), d.a.tocher@ucl.ac.uk (D.A. Tocher).

0022-328X/$ - see front matter © 2005 Elsevier B.V. All rights reserved.
doi:10.1016/j.jorganchem.2005.08.034

$[Os_3(CO)_{12-n}(MeCN)_n]$ ($n = 1$ or 2) with PhSeSePh afforded the 50 electron cluster $[Os_3(CO)_{10}(\mu\text{-SePh})_2]$ in which one SePh group bridged a closed Os–Os edge and the other an open Os–Os edge. Recently, Leong and Zhang [15] reported the corresponding tellurium analog $[Os_3(CO)_{10}(\mu\text{-TePh})_2]$ from the reaction between $[Os_3(CO)_{10}(MeCN)_2]$ and PhTeTePh. Thermolysis of both $[Os_3(CO)_{10}(\mu\text{-SePh})_2]$ and $[Os_3(CO)_{10}(\mu\text{-TePh})_2]$ at 80 °C was reported to lead to an isomer in which both the EPh (E = Se, Te) moieties bridge the same open metal–metal edge.

The reactions of the bridging dppm triosmium cluster $[Os_3(CO)_{10}(\mu\text{-dppm})]$ (**1**) with a variety of small inorganic and organic ligands have been reported to give many interesting molecules because of the ability of the dppm ligand to keep the metal cluster fragment intact during chemical reactions [16]. However, there are examples in which the diphosphine ligands can undergo C–H and P–C bond cleavage and M–H and M–C bond forming reactions [17,18]. We have previously reported [19] the reaction of $[Os_3(CO)_{10}(\mu\text{-dppm})]$ with PhSeSePh at 110 °C, which allows isolation of the binuclear compound $[Os_2(CO)_4(\mu\text{-SePh})_2(\mu\text{-dppm})]$, three 50 electron isomeric compounds with formula $[Os_3(CO)_8(\mu\text{-SePh})_2(\mu\text{-dppm})]$ and the benzyne compound $[Os_3(CO)_6(\mu\text{-CO})(\mu\text{-Se})_2(\mu\text{-}C_6H_4)(\mu\text{-dppm})]$. Herein, we report our results on the investigations of the reactions of **1** with PhSSPh and PhTeTePh in order to understand the impact of the nature of the calcogenide on the structure of the products obtained.

2. Results and discussion

The reaction of $[Os_3(CO)_{10}(\mu\text{-dppm})]$ (**1**) with two equivalents of diphenyldisulfide in refluxing toluene, followed by chromatographic separation, gave three new compounds $[(\mu\text{-H})Os_3(CO)_7(\mu\text{-SPh})\{\mu_3\text{-}\eta^4\text{-}Ph_2PCHP(Ph)C_6H_4\}]$ (**2**), $[Os_3(CO)_8(\mu\text{-SPh})_2(\mu\text{-dppm})]$ (**3**) and $[(\mu\text{-H})Os_3(CO)_7(\mu\text{-}\eta^2\text{-}SC_6H_4)(\mu\text{-SPh})(\mu\text{-dppm})]$ (**4**) in 20%, 21% and 26% yields, respectively (Scheme 1). The compounds have been characterized by elemental analysis, IR, ^1H NMR, $^{31}P\{^1H\}$NMR, mass spectroscopic data together with single crystal X-ray diffraction studies for **2** and **3**.

The molecular structure of **2** is shown in Fig. 1, crystal data are given Table 1 and selected bond distances and angles are given in Table 2. The Os_3 core in **2** represents a scalene triangle with three distinctly different Os–Os bond lengths {Os(1)–Os(2) = 3.0523(3), Os(2)–Os(3) = 2.8995(3) and Os(1)–Os(3) = 2.8495(3) Å}. These bond lengths are

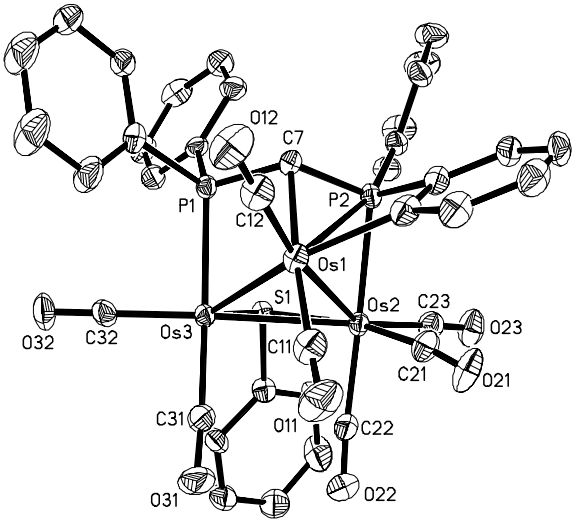

Fig. 1. Solid-state molecular structure of $[(\mu\text{-H})Os_3(CO)_7(\mu\text{-SPh})(\mu_3\text{-}\eta^4\text{-}Ph_2PCHPhPC_6H_4)]$ (**2**). Thermal ellipsoids are drawn at 50% probability level.

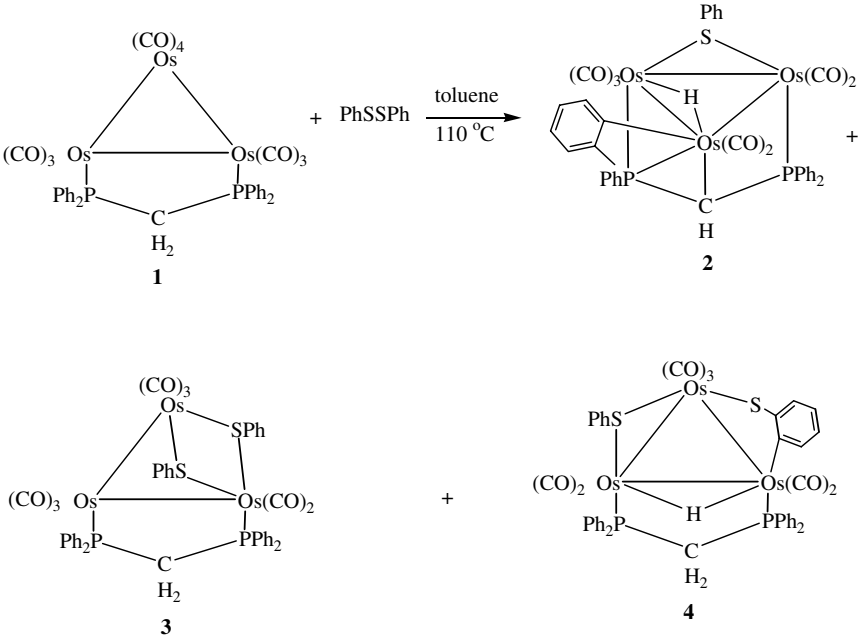

Scheme 1.

Table 1
Crystallographic data and structure refinement for **2**, **3** and **7**

	2	**3** · H_2O · H_2S	**7**
Formula	$C_{38}H_{25}O_7Os_3P_2S$	$C_{45}H_{36}O_9Os_3P_2S_3$	$C_{45}H_{32}O_8Os_3P_2Te_2$
Formula weight	1258.18	1449.46	1588.45
Temperature (K)	293(2)	150(2)	150(2)
Crystal system	Triclinic	Triclinic	Orthorhombic
Space group	$P\bar{1}$	$P\bar{1}$	*Pbca*
a (Å)	10.3719(5)	11.9787(2)	21.6362(11)
b (Å)	11.7890(5)	12.3035(2)	18.0333(9)
c (Å)	16.6625(8)	16.9587(3)	22.8700(12)
α (°)	78.3540(10)	94.2600(10)	90
β (°)	76.3130(10)	97.7520(10)	90
γ (°)	66.9870(10)	107.7820(10)	90
V (Å^3)	1808.33(14)	2340.49(7)	8923.2(8)
Z	2	2	8
D_{calc} (mg m^{-3})	2.311	2.057	2.365
μ (Mo Kα) (mm^{-1})	10.710	8.378	9.928
F(000)	1166	1368	5824
Crystal size (mm)	0.36 × 0.18 × 0.05	0.25 × 0.20 × 0.12	0.23 × 0.14 × 0.04
θ range (°)	1.89–28.31	2.93–27.49	1.72–28.32
Limiting indices	$-13 \leqslant h \leqslant 13$, $-15 \leqslant k \leqslant 15$, $-22 \leqslant l \leqslant 22$	$-15 \leqslant h \leqslant 15$, $-15 \leqslant k \leqslant 15$, $-21 \leqslant l \leqslant 22$	$-28 \leqslant h \leqslant 27$, $-23 \leqslant k \leqslant 23$, $-30 \leqslant l \leqslant 30$
Number of reflections collected	16106	43599	76686
Number of independent reflections [R_{int}]	8386 [0.0339]	10668 [0.0949]	10912 [0.0615]
Max. and min. trans.	0.6165 and 0.1134	0.4330 and 0.2285	0.6922 and 0.2086
Data/restraints/parameters	8386/0/460	10668/0/568	10912/0/541
Goodness-of-fit on F^2	1.026	1.052	1.177
Final *R* indices [$I > 2\sigma(I)$]	$R_1 = 0.0316$, $wR_2 = 0.0782$	$R_1 = 0.0465$, $wR_2 = 0.01147$	$R_1 = 0.0365$, $wR_2 = 0.0665$
R indices (all data)	$R_1 = 0.0344$, $wR_2 = 0.0799$	$R_1 = 0.0648$, $wR_2 = 0.1245$	$R_1 = 0.0439$, $wR_2 = 0.0686$
Largest diff. peak and hole (e Å^{-3})	3.311 and −2.279	2.440 and −2.628	1.283 and −1.198

Table 2
Selected bond distances (Å) and angles (°) for [(μ-H)Os_3(CO)$_7$(μ-SPh)(μ$_3$-η^4-Ph_2PCHPhPC_6H_4)] (**2**)

Os(1)–C(12)	1.854(5)
Os(1)–C(71)	2.080(5)
Os(1)–Os(3)	2.8495(3)
Os(1)–Os(2)	3.0523(3)
Os(2)–C(23)	1.933(5)
Os(2)–P(2)	2.4085(11)
Os(2)–Os(3)	2.8995(3)
Os(3)–C(31)	1.908(5)
Os(3)–P(1)	2.3736(11)
Os(1)–C(11)	1.893(5)
Os(1)–C(7)	2.240(4)
Os(1)–P(2)	2.8504(11)
Os(2)–C(21)	1.913(5)
Os(2)–C(22)	1.941(5)
Os(2)–S(1)	2.4528(11)
Os(3)–C(32)	1.875(5)
Os(3)–S(1)	2.3619(11)
S(1)–C(1)	1.789(5)
C(71)–Os(1)–Os(3)	143.14(13)
C(71)–Os(1)–Os(2)	87.30(13)
P(2)–Os(2)–Os(3)	90.32(3)
Os(3)–Os(2)–Os(1)	57.140(6)
P(1)–Os(3)–Os(2)	92.30(3)
P(1)–C(7)–P(2)	118.3(2)
C(71)–Os(1)–C(7)	81.00(18)
Os(3)–Os(1)–Os(2)	58.730(6)
S(1)–Os(2)–Os(3)	51.55(3)
S(1)–Os(3)–Os(2)	54.42(3)
Os(3)–S(1)–Os(2)	74.03(3)
Os(1)–Os(3)–Os(2)	64.130(7)

all in accord with other documented Os–Os single bond lengths. The fact that the Os(1)–Os(2) bond length is significantly longer than the Os(2)–Os(3) and Os(1)–Os(3) edges provides support for the presence of the bridging hydride on this edge [20] and this also makes the individual metal centers electron- precise. The seven carbonyl ligands are all in terminal positions with two linked to osmium atoms Os(1) and Os(3) and three linked to Os(2). The most striking feature of the structure is that the dppm ligand has been transformed into a unique μ$_3$-η^4-Ph_2PCHP(Ph)C_6H_4 coordination mode with two phosphorus atoms coordinating axially at the Os(2)–Os(3) edge. The C(7) atom of the methylene of the dppm ligand occupies an axial coordination site on Os(1). The structure shows that two kinds of C–H activation, orthometallation of one of the phenyl groups as well as the unusual activation of the methylene group of the dppm ligand occur in the transformation. Thermolysis of [Os_3(CO)$_9$(CNPr)(μ-dppm)] in refluxing toluene has been reported to produce [(μ-H)$_2Os_3$(CO)$_7$(CNR){μ$_3$-η^4-Ph_2PCHP(Ph)C_6H_4}], containing a μ$_3$,η^4-Ph_2PCHP(Ph)-C_6H_4 ligand [17] and this appears to be the second example of this coordination of the diphosphine ligand on a triosmium center. The μ$_3$-η^4-Ph_2PCHP(Ph)C_6H_4 ligand in **2** is bonded to three osmium atoms through P(1), P(2), C(7) and C(71) atoms (Os(3)–P(1) = 2.3736(11), Os(2)–P(2) = 2.4085(11), Os(1)–C(7) = 2.240(4), and Os(1)–C(71) = 2.080(5) Å) leading to two four-membered and one five-membered metallocycles, Os(1)–C(7)–P(1)–Os(3), Os(1)–

C(7)–P(1)–Os(3), and Os(2)–P(2)–C(7)–P(1)–Os(2). Another interesting feature of the structure is that the two phosphorus atoms of the diphosphine ligand are coordinating axially at the Os(2)–Os(3) vector and the Os–P bond distances are significantly longer than those reported for the orthometallated compound $[(\mu\text{-H})Os_3(CO)_8\{Ph_2PCH_2\text{-}P(Ph)C_6H_4\}]$ [16b]. Another feature of interest in **2** is the μ-SPh group which asymmetrically spans the Os(2)–Os(3) edge {Os(2)–S(1) = 2.4528(11) and Os(3)–S(1) = 2.3619(11) Å} and the average Os–S bond distance {2.407(2) Å} is similar to that observed in $[(\mu\text{-H})Os_3(CO)_8\text{-}(\mu\text{-SEt})(\mu\text{-dppm})]$ although the thiolato group in the latter is symmetrically bridged [21].

Spectroscopic data in solution for **2** are in agreement with the structure observed in solid-state. Compound **2** exhibits IR bands due to terminal carbonyl ligands only. The hydride region of the ^{1}H NMR spectrum of **2** shows a doublet at δ −15.0 with a phosphorus–hydrogen coupling constant of 18.0 Hz. In addition to the phenyl resonances of the dppm ligand the ^{1}H NMR spectrum in the aliphatic region contains a double doublets at δ 5.14 with P–H coupling constants of 10.4 and 3.2 Hz which integrated for one proton and is assigned to the CH group of dppm, suggesting that one of the methylene hydrogens has been activated. The ^{31}P {^{1}H} NMR spectrum of **2** contains two doublets at δ −18.4 and −28.7 (J = 91.4 Hz), indicating non-equivalent ^{31}P nuclei. The fused rings in **2** are connected by edge sharing and severe twist of the rings suggests unusual ring size effect of the μ_3-η^4-coordinated dppm ligand and reflects up field ^{31}P chemical shifts of the phosphorus atoms. The FAB mass spectrum shows the molecular ion peak at *m/z* 1260 and ions due to the subsequent loss of seven carbonyl ligands.

The molecular structure **3** is shown in Fig. 2, crystal data and structure refinement parameters are given in Table 1 and selected bond distances and angles are given in Table 3. The molecule consists of an open cluster of three osmium atoms with two almost equal metal–metal bonds {Os(1)–Os(2) = 2.9273(4) and Os(2)–Os(3) = 2.8915(4) Å}, eight terminal carbonyl groups, two bridging phenylsulfide groups and a bridging dppm ligand. Among the eight carbonyl ligands, three each are bonded to the two osmium atoms Os(2) and Os(3) and two are bonded to Os(1). The Os(1)–Os(2) edge is bridged by the dppm ligand and the open Os(1)...Os(3) edge is symmetrically bridged by two SPh groups {Os(1)–S(1) = 2.4515(18), Os(3)–S(1) = 2.4434(19); Os(1)–S(2) = 2.443(2) and Os(3)–S(2) = 2.4339(19) Å}. The Os–P bond distances {Os(1)–P(1) = 2.324(2) and Os(2)–P(2) = 2.336(2) Å} are very similar to those reported for **1** {2.332(3) and 2.324(7) Å} [22]. The overall structure of **3** is similar to that of the Se analog $[Os_3(CO)_8(\mu\text{-SePh})_2\text{-}(\mu\text{-dppm})]$ which was synthesized from the reaction of **1** with PhSeSePh and cha-racterized by a single crystal X-ray diffraction analysis [19].

The spectroscopic data for **3** are consistent with the solid-state structure. The pattern of the infrared spectrum of **3** is very similar to that observed for $[Os_3(CO)_8(\mu\text{-SePh})_2\text{-}(\mu\text{-dppm})]$ [19]. The ^{1}H NMR spectrum of **3** displays the expected signals for the dppm and SPh ligands, while the ^{31}P {^{1}H} NMR spectrum exhibits two doublets at δ 20.8

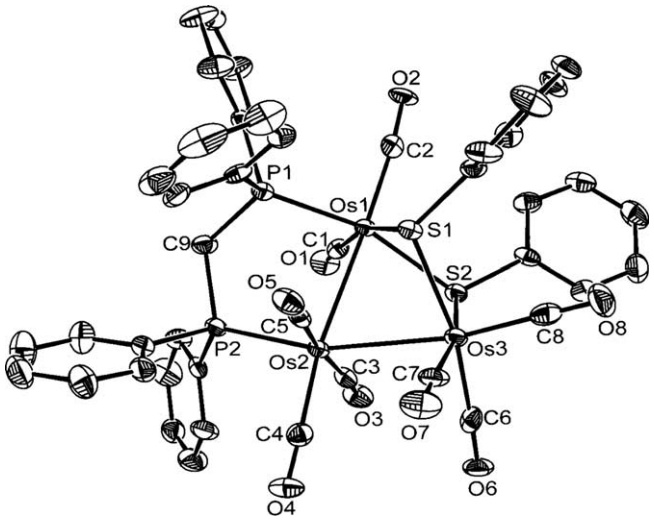

Fig. 2. Solid-state molecular structure of $[Os_3(CO)_8(\mu\text{-SPh})_2(\mu\text{-dppm})]$ (**3**). Thermal ellipsoids are drawn at 50% probability level.

Table 3
Selected bond distances (Å) and angles (°) for $[Os_3(CO)_8(\mu\text{-SPh})_2(\mu\text{-dppm})]$ (**3**)

Os(1)–C(1)	1.891(8)
Os(1)–P(1)	2.324(2)
Os(1)–S(1)	2.4515(18)
Os(2)–C(4)	1.895(8)
Os(2)–C(5)	1.954(8)
Os(2)–Os(3)	2.8915(4)
Os(3)–C(8)	1.904(9)
Os(3)–S(2)	2.4339(19)
P(1)–C(9)	1.820(8)
S(1)–C(34)	1.800(8)
Os(1)–C(2)	1.906(11)
Os(1)–S(2)	2.443(2)
Os(1)–Os(2)	2.9273(4)
Os(2)–C(3)	1.943(9)
Os(2)–P(2)	2.336(2)
Os(3)–C(7)	1.903(9)
Os(3)–C(6)	1.907(9)
Os(3)–S(1)	2.4434(19)
P(1)–C(9)	1.833(8)
S(2)–C(40)	1.786(8)
P(1)–Os(1)–S(2)	164.08(6)
S(2)–Os(1)–S(1)	82.56(6)
S(2)–Os(1)–Os(2)	79.70(4)
P(2)–Os(2)–Os(1)	90.97(5)
S(2)–Os(3)–S(1)	82.91(6)
S(1)–Os(3)–Os(2)	76.51(4)
Os(3)–S(2)–Os(1)	89.65(7)
P(1)–Os(1)–S(1)	97.89(7)
P(1)–Os(1)–Os(2)	84.98(5)
S(1)–Os(1)–Os(2)	75.71(4)
Os(3)–Os(2)–Os(1)	72.427(10)
S(2)–Os(3)–Os(2)	80.58(5)
Os(3)–S(1)–Os(1)	89.23(6)
P(1)–C(9)–P(2)	113.9(4)

and 17.3 ($J = 69.8$ Hz) corresponding to two non-equivalent ^{31}P nuclei. The FAB mass spectrum shows the molecular ion peak at *m/z* 1398 and fragmentation peaks due to the sequential loss of eight carbonyl ligands.

The infrared spectrum of **4** shows all the carbonyl groups are terminal. In addition to the usual phenyl proton resonances the aromatic region of the ^1H NMR spectrum of **4** contains four well separated signals, two doublets at δ 7.82 ($J = 8.0$ Hz) and 7.72 ($J = 8.0$ Hz) and two triplets at δ 7.61($J = 8.0$ Hz) and 7.21 ($J = 8.0$ Hz) each integrating for one hydrogen. The doublets at δ 7.82 and 7.72 are assigned to the protons on C(3) and C(6) interchangably while the triplets at δ 7.61 and 7.21 are due to the protons on C(4) and C(5) interchangeably. The aliphatic region of the spectrum contains two multiplets at δ 3.10 and 1.71 due to the methylene protons of the dppm ligand. The hydride region of the spectrum exhibits a triplet at δ −15.55. The ^{31}P $\{^1H\}$ NMR spectrum contains two doublets at δ 20.8 and 17.3 due to two non-equivalent ^{31}P nuclei. The FAB mass spectrum exhibits the molecular ion peak at *m/z* 1370 and ions due to the sequential loss of seven carbonyl ligands. These data are consistent with the structure of **4** shown in Scheme 1.

It is reasonable to propose that compound **3** is an intermediate in the formation of **2** and **4**. To support this, we have investigated the thermolysis of both **3** and **4** at different temperatures. Thermolysis of **3** in refluxing toluene for 3 h produces **4** by loss of one CO ligand following activation of a C–H bond of one SPh ligand. As expected, thermolysis of **4** in refluxing octane leads to the formation of **2** by loss of a thiophenol molecule. Given these results it seems reasonable to propose that **3** loses thiophenol and that one of the subsequent C–H activations which result in the formation of **2** is coupled to a reductive elimination of one C–H on the sulfur bound phenyl group.

The reaction of **1** with two equivalents of diphenylditelluride in refluxing toluene gave the binuclear compound $[Os_2(CO)_4(\mu\text{-TePh})_2(\mu\text{-dppm})]$ (**6**) in 15% yield, and two 50 electron isomeric compounds **5** and **7** with the formula $[Os_3(CO)_8(\mu\text{-TePh})_2(\mu\text{-dppm})]$ in 20%, and 23% yields, respectively (Scheme 2). We were unable to obtain X-ray quality crystals of **5** and **6**, therefore their characterization is based on elemental analysis, infrared, ^1H NMR, $^{31}P\{^1H\}$ NMR and mass spectroscopic data. Compound **7** has been characterized by a combination of spectroscopic data and single crystal X-ray diffraction analysis. For **5**, IR carbonyl stretching bands at 2058 vs, 2014 m, 1983 vs, and 1935 w cm^{-1} indicate that only terminal carbonyl groups are present in the molecule. The mass spectrum of **5** exhibits a molecular ion peak at *m/z* 1590 and sequential loss of eight carbonyls groups were observed. In addition to the usual phenyl protons for the dppm and TePh ligands the ^1H NMR spectrum of **5** shows two multiplets at δ 4.78 and 4.48 due to the methylene protons of the dppm ligand. The $^{31}P\{^1H\}$ NMR spectrum of **5** contains two doublets at δ 4.1 and −5.6 ($J = 74.6$ Hz) due to the two non-equivalent ^{31}P nuclei. These data are consistent with proposed structure for **5** with dppm and TePh groups bridging at different Os–Os edge of osmium triangle.

Compound **6** has also been characterized spectroscopically. The binuclear formulation of **6** was indicated by its elemental analysis and mass spectrum which exhibits the molecular ion peak at *m/z* 1288 and ions due to the sequential loss of four carbonyls groups. The infrared spectrum contains three ν(CO) bands at 2016 vs, 1993 s, and 1927 m cm^{-1}, a very similar IR spectrum to that observed for $[Os_2(CO)_2(\mu\text{-SePh})_2(\mu\text{-dppm})]$ which was characterized by a single crystal X-ray diffraction studies.[19] In addition to phenyl resonances for the dppm and TePh ligands at δ 8.15–6.98 the ^1H NMR spectrum of **6** shows two multiplets

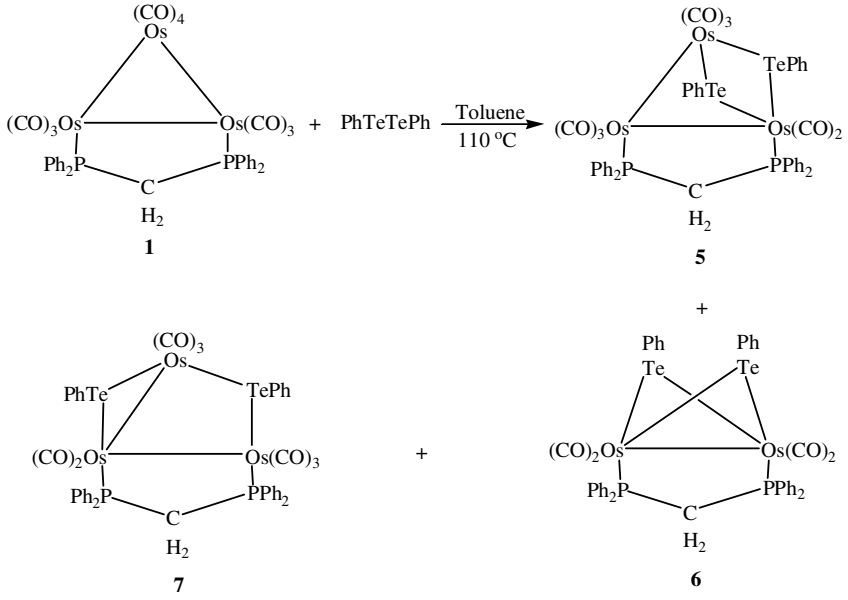

Scheme 2.

at δ 4.77 and 4.58 due to the methylene protons of the dppm ligand. The $^{31}P\{^{1}H\}$ NMR spectrum shows a single peak at δ −20.8 for the two equivalent phosphorus atoms of the dppm ligand.

The molecular structure of **7** is shown in Fig. 3, crystal data and structure refinement parameters are given in Table 1 and selected bond distances and angles are given in Table 4. The molecule is a 50 electron triosmium system with two distinctly different osmium–osmium bonds, one bridging dppm and two bridging TePh ligands. The eight carbonyl ligands are all in terminal positions with two bonded to Os(3) and three bonded to each of the osmium atoms Os(1) and Os(2). The structure is derived from that of $[Os_3(CO)_{10}(\mu\text{-TePh})_2]$ by replacement of an equatorial carbonyl group on each of the two osmium atoms of the non-bridged Os–Os edge with the dppm ligand [15]. The open Os(1)–Os(2) edge 4.12 Å is symmetrically bridged by one TePh ligand, and the other TePh ligand symmetrically spans the Os(2)–Os(3) edge, while the dppm ligand bridges the Os(1)–Os(3) edge. The Os–Te bond distances {Os(1)–Te(1) = 2.6946(4), Os(2)-Te(1) = 2.7110(4), Os(2)–Te(2) = 2.6724(4) and Os(3)–Te(2) = 2.6821(4) Å} are comparable to those observed in $[Os_3(CO)_{10}(\mu\text{-TePh})_2]$ {2.7274(9)–2.6886(10) Å} [15]. The Os(1)–Te(1)–Os(2) angle {99.215(13)°} involving the open Os–Os edge is significantly larger than the Os(2)–Te(2)–Os(3) angle {65.686(10)} involving the bridged Os–Os edge. The dppm bridged Os(1)–Os(3) edge {3.0197(3) Å} is significantly longer than that of the Os(2)–Os(3) edge {2.9040(3) Å) and the dppm bridging edge in **1** {2.8712(8) Å}. The Os–P bond lengths {Os(3)–P(2) = 2.3256(14) and Os(1)–P(1) = 2.3225(14) Å} are very similar to those observed for **3** and **1**.

The spectroscopic data for **7** are consistent with the solid-state structure. The pattern of the infrared spectrum is similar to that of the Se analog $[Os_3(CO)_8(\mu\text{-SePh})_2(\mu\text{-dppm})$. The mass spectrum exhibits the molecular ion peak at *m/z* 1590 and fragmentation peaks due to the sequential loss of eight carbonyl ligands. In addition to the phenyl resonances for the dppm and TePh ligands the ^{1}H NMR spectrum shows a overlapping multiplets at δ 4.35 integra- ting for two hydrogen atoms due to the methylene protons of the dppm ligand. The $^{31}P\{^{1}H\}$ NMR spectrum contains two doublets at δ 14.1 and 4.2 with phosphorus–phosphorus coupling constant of 81.2 Hz, indicating non-equivalent ^{31}P nuclei.

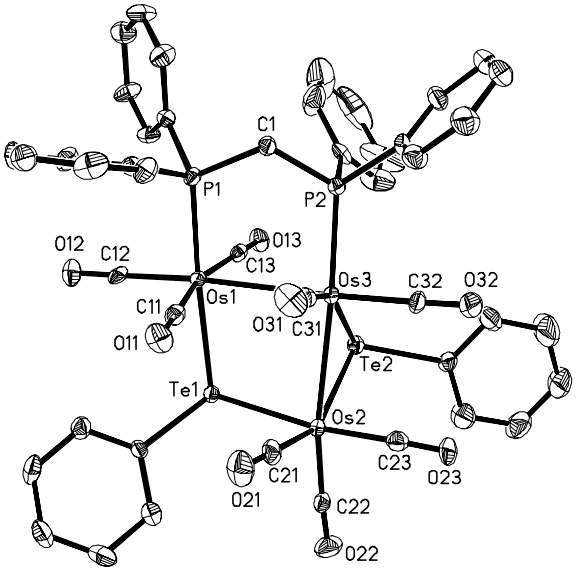

Fig. 3. Solid-state molecular structure of $[Os_3(CO)_8(\mu\text{-TePh})_2(\mu\text{-dppm})]$ (**7**). Thermal ellipsoids are drawn at 50% probability level.

Table 4
Selected bond distances (Å) and angles (°) for $[Os_3(CO)_8(\mu\text{-TePh})_2(\mu\text{-dppm})]$ (**7**)

Os(1)–C(12)	1.903(6)
Os(1)–C(13)	1.935(6)
Os(1)–Te(1)	2.6946(4)
Os(2)–C(23)	1.886(7)
Os(2)–C(22)	1.903(6)
Os(2)–Te(1)	2.7110(4)
Os(3)–C(31)	1.863(6)
Os(3)–P(2)	2.3256(14)
Te(1)–C(41)	2.133(5)
Os(1)–C(11)	1.951(6)
Os(1)–P(1)	2.3325(14)
Os(1)–Os(3)	3.0197(3)
Os(2)–C(21)	1.900(6)
Os(2)–Te(2)	2.672494)
Os(2)–Os(3)	2.9040(3)
Os(3)–C(32)	1.869(6)
Os(3)–Te(2)	2.6821(4)
Te(2)–C(51)	2.131(6)
Te(1)–Os(1)–Os(3)	84.033(10)
P(1)–Os(1)–Os(3)	91.62(4)
Te(2)–Os(2)–Os(3)	57.317(10)
P(2)–Os(3)–Te(2)	110.47(4)
Te(2)–Os(3)–Os(2)	56.997(10)
Te(2)–Os(3)–Os(1)	90.054(11)
Os(2)–Te(2)–Os(3)	65.686(10)
P(1)–Os(1)–Te(1)	175.43(4)
Te(2)–Os(2)–Te(2)	79.114(12)
Te(1)–Os(2)–Os(3)	86.013(10)
P(2)–Os(3)–Os(2)	165.74(4)
P(2)–Os(3)–Os(1)	85.05(4)
Os(1)–Te(1)–Os(2)	99.215(13)
P(1)–C(1)–P(2)	113.2(3)

3. Conclusions

Having now completed the studies of the reactions of the entire chalcogenide triad of PhEEPh with **1** a few general conclusions can be made. The larger members of the triad Se and Te clearly lead to more Os–Os bond opening and even to fragmentation of the cluster in spite of the presence of the dppm ligand, which in general tends to hold the osmium triangle together. The diphenyldisulfide on the other hand with its smaller chalcogenide atom leads ultimately only to closed trinuclear products. However, in the case of the more sterically encumbered dppm derivative the product resulting from initial oxidative addition of he S–S bond to the cluster is less stable than the parent carbonyl complex and leads to reductive elimination of thiophenol and to subsequent C–H activation processes

involving both the SPh and dppm ligands, in order to satisfy the electronic requirements of the cluster. These conclusions should prove useful in utilizing this synthetic approach for cluster condensation reactions and for modeling heterogeneous catalyst systems.

4. Experimental

Unless otherwise stated, all reactions were carried out under nitrogen atmosphere using standard Schlenk techniques. Reagent grade solvents were dried and distilled prior to use by standard methods. Infrared spectra were recorded on a Shimadzu FT-IR 8101 spectrophotometer. ^{1}H and ^{31}P{^{1}H} NMR spectra were recorded on a Varian Unity Plus 400 spectrometer. Chemical shifts for the ^{31}P{^{1}H} NMR spectra are relative to 85% H_3PO_4. Elemental analyses were carried out by the Microanalytical Laboratory at University College London. Fast atom bombardment mass spectra were obtained on a JEOL SX-102 spectrometer using 3-nitrobenzyl alcohol as matrix and CsI as calibrant. Diphenyldisulfide and diphenylditelluride were purchased from Aldrich and used as received. The starting compound $[Os_3(CO)_{10}(\mu\text{-dppm})]$ was prepared according to the published procedure [16c].

4.1. Reaction of $[Os_3(CO)_{10}(\mu\text{-dppm})]$ (1) with PhSSPh

A toluene solution (25 mL) of $[Os_3(CO)_{10}(\mu\text{-dppm})]$ (0.105 g, 0.085 mmol) and PhSSPh (0.038 g, 0.174 mmol) was heated to reflux at 110 °C for 3 h during which time the color changed from yellow to orange. The solvent was removed under reduced pressure and residue chromatographed by TLC on silica gel. Elution with hexane/CH_2Cl_2 (7:3, v/v) developed three bands. The first band afforded $[(\mu\text{-H})Os_3(CO)_7(\mu\text{-SPh})\{\mu_3\text{-}\eta^4\text{-}Ph_2PCHP(Ph)C_6H_4\}]$ (**2**) (0.021 g, 20%) as orange crystals after recrystallization from hexane/CH_2Cl_2 at −20 °C (Anal. Calc. for $C_{38}H_{26}O_7Os_3P_2S$: C, 36.24; H, 2.08. Found: C, 36.46; H, 2.22%). IR (νCO, CH_2Cl_2): 2080 s, 2012 vs, 1997 s, 1973 w, 1943 w, 1925 m cm^{-1}; ^{1}H NMR (CD_2Cl_2): δ 8.07–6.13 (m, 24H), 5.14 (dd, 1H, d, $J = 10.4$, 3.2 Hz), −15.0 (d, $J = 18.0$ Hz); ^{31}P{^{1}H} NMR($CDCl_3$): δ −18.4 (d, $J = 91.4$ Hz), −28.7 (d, $J = 91.4$ Hz); MS (FAB): *m/z* 1260 (M^+). The second band gave $[Os_3(CO)_8(\mu\text{-SPh})_2(\mu\text{-dppm})]$ $\mathbf{3}\cdot H_2O\cdot H_2S$ (0.026 g, 21%) as yellow crystals from hexane/CH_2Cl_2 at −20 °C (Anal. Calc. for $C_{45}H_{36}O_9Os_3P_2S_3$: C, 37.28; H, 2.50. Found: C, 37.53; H, 2.72%). IR (νCO, CH_2Cl_2): 2070 s, 2026 m, 1993 vs, 1968 w, 1943 w cm^{-1}; ^{1}H NMR(CD_2Cl_2): δ 7.83–7.05 (m, 30H), 5.03 (m. 1H), 4.65 (m. 1H); ^{31}P{^{1}H} NMR(CD_2Cl_2): δ 17.3 (d, $J = 69.8$ Hz), 20.8 (d, $J = 69.8$ Hz); FAB MS: *m/z* 1398 (M^+). The third band afforded $[(\mu\text{-H})Os_3(CO)_7(\mu,\eta^2\text{-}SC_6H_4)(\mu\text{-SPh})(\mu\text{-dppm})]$ (**4**) (0.029 g, 26%) as pale yellow crystal after recrystallization from hexane/CH_2Cl_2 at −20 °C. (Anal. Calc. for $C_{44}H_{32}O_7Os_3P_2S_2$: C, 38.59; H, 2.36. Found: C, 38.83; H, 2.72%). IR (νCO, CH_2Cl_2): 2056 m, 2041 vs, 1997 w, 1983 s, 1956 w cm^{-1}; ^{1}H NMR (CD_2Cl_2): δ 7.50–6.76(m, 25H), 7.82 (d, 1H, $J = 8.0$ Hz), 7.72 (d, 1H, $J = 8.0$ Hz), 7.61($J = 8.0$ Hz), 7.21 ($J = 8.0$ Hz) 3.10 (m. 1H), 1.71(m, 1H), −15.55 (t, $J = 8.2$ Hz); ^{31}P{^{1}H} NMR-(CD_2Cl_2): δ 20.8 (d, $J = 91.4$ Hz)), 17.3 (d, $J = 91.4$ Hz); FAB MS: *m/z* 1370 (M^+).

4.2. Thermolysis of 3

(a) A toluene solution of **3** (0.015 g, 0.011 mmol) was heated to reflux under nitrogen for 4 h. Workup and chromatographic separation as above afforded **4** (0.008 g, 53%).
(b) A similar thermolysis of **3** (0.015 g, 0.011 mmol) in refluxing octane for 2 h followed by similar chromatographic separation gave **2** (0.009 g, 50%).

4.3. Thermolysis of 4

An octane solution of **4** (0.015 g, 0.009 mmol) was heated to reflux for 1.5 h. Workup and chromatographic separation as above afforded **2** (0.005 g, 45%).

4.4. Reaction of 1 with PhTeTePh

A toluene solution (25 mL) of **1** (0.100 g, 0.081 mmol) and PhTeTePh (0.066 g, 0.161 mmol) was refluxed for 3 h. The solvent was removed under reduced pressure and the residue chromatographed by TLC on silica gel. Elution with hexane/CH_2Cl_2 (2:1, v/v) developed three bands. The first band afforded $[Os_3(CO)_8(\mu\text{-TePh})_2(\mu\text{-dppm})]$ (**5**) (0.026 g, 20%) as yellow crystals after recrystallizaton from hexane/CH_2Cl_2 at −20 °C (Anal. Calc. for $C_{45}H_{32}O_8Os_3P_2Te_2$: C, 34.02; H, 2.03. Found: C, 34.33; H, 2.32%). IR (νCO, CH_2Cl_2): 2058 s, 2014 m, 1983 vs, 1958 w, 1935 w cm^{-1}; ^{1}H NMR(CD_2Cl_2): δ 7.58–6.55 (m, 30H), 4.78 (m. 1H), 4.48 (m, 1H);^{31}P{^{1}H} NMR(CD_2Cl_2): δ 4.1 (d, $J = 74.6$ Hz)), −5.6 (d, $J = 74.6$ Hz); FAB MS: *m/z* 1590. The second band yielded $[Os_2(CO)_4(\mu\text{-TePh})_2(\mu\text{-dppm})]$ (**6**) (0.016 g, 15%) as red crystals from hexane/CH_2Cl_2 at −20 °C (Anal. Calc. for $C_{41}H_{32}O_4Os_2P_2Te_2$: C, 38.28; H, 2.51. Found: C, 34.45; H, 2.76%). IR (νCO, CH_2Cl_2): 2016 vs, 1993 s, 1927 m cm^{-1}; ^{1}H NMR(CD_2Cl_2): δ 8.15–6.98 (m, 30H), 4.77 (m. 1H), 4.58 (m, 1H);^{31}P{^{1}H} NMR(CD_2Cl_2): δ −20.8 (s); FAB MS: *m/z* 1288. The third band afforded $[Os_3(CO)_8(\mu\text{-TePh})_2(\mu\text{-dppm})]$ (**7**) (0.030 g, 23%) as orange crystals after recrystallizaton from hexane/CH_2Cl_2 at −20 °C (Anal. Calc. for $C_{45}H_{32}O_8Os_3P_2Te_2$: C, 34.02; H, 2.03. Found: C, 34.41; H, 2.36%). IR (νCO, CH_2Cl_2): 2053 s, 2031 s, 1972 s cm^{-1}; ^{1}H NMR(CD_2Cl_2): δ 7.78–7.18 (m, 30H), 4.35 (m, 2H); ^{31}P{^{1}H} NMR-(CD_2Cl_2): δ 14.1 (d, $J = 81.2$ Hz), 4.2 (d, $J = 81.2$ Hz); FAB MS: *m/z* 1590.

4.5. X-ray crystallography for compounds 2, 3, and 7

Intensity data for **3** were obtained using a Bruker Nonius Kappa CCD diffractometer using Mo Kα radiation.

Data collection and processing were carried out by using the programs COLLECT [23] and DENZO [24]. Data were corrected for absorption effects using SORTAV [25]. Data for complexes **2** and **7** were obtained on a Bruker SMART APEX CCD diffractometer using Mo Kα radiation. Data reduction and integration were carried out with SAINT+ and absorption corrections using SADABS [26].

The structures were solved by direct methods and refined on F^2 by full-matrix least squares (SHELXTL PLUS V6.10) [26] using all unique data. For all structures, the non-hydrogen atoms were refined anisotropically and the hydrogen atoms were included in calculated positions (riding model). The crystal data, details of data collection and refinement results are summarized in Table 1.

Acknowledgments

Part of this work was carried out by SEK at University College London. He gratefully acknowledges the Royal Society (London) for a fellowship to spend time at UCL.

Appendix A. Supplementary data

Crystallographic data have been deposited with the Cambridge Crystallographic Data Centre, CCDC Nos. 278326 for **2**, 278327 for **3**, and 278328 for **7**. Copies of this information may be obtained free of charge from the Director, CCDC, 12 Union Road, Cambridge, CB2 1EZ, UK (fax: +44 1223 336 033, email deposit@ccdc.cam.ac.uk or WWW: www.ccdc.cam.ac.uk). Supplementary data associated with this article can be found, in the online version, at doi:10.1016/j.jorganchem.2005.08.034.

References

[1] (a) A. Hill, R. West, Adv. Organomet. Chem. 41 (1997) 243;
(b) R. Philip, G.R. Kumar, P. Mathur, S. Ghose, Opt. Commun. 178 (2000) 469.
[2] P. Braunstein, C. Graiff, C. Massera, G. Predieri, J. Rose, A. Tiripicchio, Inorg. Chem. 41 (2002) 1372.
[3] M. Shieh, H.-S. Chen, Y.-W. Lai, Organometallics 23 (2004) 4018.
[4] M.L. Kuhlman, T.B. Rauchfuss, Organometallics 23 (2004) 5085.
[5] M. Shieh, M.-H. Hsu, J. Cluster Sci. 15 (2004) 91.
[6] R.D. Adams, M. Tasi, J. Cluster Sci. 1 (1990) 249.
[7] R.D. Adams, Polyhedron 4 (1985) 2003.
[8] S.E. Kabir, S. Pervin, N.C. Sarker, A. Yesmin, A. Sharmin, T.A. Siddiquee, D.T. Haworth, D.W. Bennett, K.M.A. Malik, J. Organomet. Chem. 681 (2003) 237.
[9] T. Akter, N. Begum, A. Yesmin, D.T. Haworth, D.W. Bennett, S.E. Kabir, Md.A. Miah, N.C. Sarker, T.A. Siddiquee, E. Rosenberg, J. Organomet. Chem. 689 (2004) 237.
[10] (a) D. Cauzzi, C. Graiff, C. Massera, G. Mori, G. Predieri, A. Tiripicchio, J. Chem. Soc., Dalton Trans. (1998) 321;
(b) D. Cauzzi, C. Graiff, G. Predieri, A. Tiripicchio, C. Vignali, J. Chem. Soc., Dalton Trans. (1999) 237.
[11] D. Cauzzi, C. Graiff, G. Predieri, A. Tiripicchio, in: P. Baistrocchi, L.A. Oro, P.R. Raitby, A. Tiripicchio (Eds.), Metal Clusters in Chemistry, vol. 1, VCH, Weinheim, 1999, pp. 193–208.
[12] I.D. Sadekov, A.I. Uraev, A.D. Garnovskii, Russ. Chem. Rev. 68 (1999) 415.
[13] P.V. Broadhurst, B.F.G. Johnson, J. Lewis, J. Chem. Soc., Dalton Trans. (1982) 1881.
[14] (a) A.J. Arce, P. Arrojo, Y.De. Sanctis, A.J. Deeming, D.J. West, Polyhedron 11 (1992) 1013;
(b) A.J. Arce, P. Arrojo, Y.De. Sanctis, A.J. Deeming, J. Chem. Soc., Chem. Commun. (1991) 1491.
[15] J. Zhang, W.K. Leong, J. Chem. Soc., Dalton Trans. (2000) 1279.
[16] (a) K.A. Azam, M.B. Hursthouse, Md.R. Islam, S.E. Kabir, K.M.A. Malik, R. Miah, C. Sudbrake, H. Vahrenkamp, J. Chem. Soc., Dalton Trans. (1998) 1097;
(b) J.A. Akter, K.A. Azam, S.E. Kabir, K.M.A. Malik, M.A. Mottalib, Inorg. Chem. Commun. 3 (2000) 553;
(c) J.A. Clucas, D.F. Foster, M.M. Harding, A.K. Smith, J. Chem. Soc., Chem. Commun. (1984) 949;
(d) D.F. Foster, J.H. Harrison, B.S. Nicholls, A.K. Smith, J. Organomet. Chem. 295 (1985) 99;
(e) S. Cartwright, J.A. Clucas, R.H. Dawson, D.F. Foster, M.M. Harding, A.K. Smith, J. Organomet. Chem. 302 (1986) 403;
(f) S.R. Hodge, B.F.G. Johnson, J. Lewis, P.R. Raithby, J. Chem. Soc., Dalton Trans. (1987) 931;
(g) B.F.G. Johnson, J. Lewis, M. Manari, D. Braga, F. Grepioni, C. Gradella, J. Chem. Soc., Dalton Trans. (1990) 2683.
[17] K.-L. Lu, H.-J. Chen, P.-Y. Lu, S.-Y. Li, F.-E. Hong, S.-M. Peng, G.-H. Lee, Organometallics 13 (1994) 585.
[18] S.E. Kabir, Md.A. Miah, N.C. Sarker, G.M.G. Hossain, K.I. Hardcastle, E. Nordlander, E. Rosenberg, Organometallics 24 (2005) 3315.
[19] S.E. Kabir, N. Begum, Md.M. Hassan, Md.I. Hyder, H. Nur, D.W. Bennett, T.A. Siddiquee, D.T. Haworth, E. Rosenberg, J. Organomet. Chem. 689 (2004) 1569.
[20] D.M.P. Mingos, D.J. Wales, Introduction to Cluster Chemistry, Prentice-Hall, Englewood Cliffs, NJ, 1990.
[21] S.M.T. Abedin, K.A. Azam, M.B. Hursthouse, S.E. Kabir, K.M.A. Malik, M.A. Mottalib, E. Rosenberg, J. Cluster Sci. 12 (2001) 5.
[22] K.A. Azam, M.B. Hursthouse, S.E. Kabir, K.M.A. Malik, M.A. Mottalib, J. Chem. Crystallogr. 29 (1999) 813.
[23] R. Hooft, COLLECT Data Collection Software, Nonius B.V., Delft, The Netherlands, 1998.
[24] Z. Otwinowski, W. Minor, in: C.W. CarterJr., R.M. Sweet (Eds.), Macromolecular Crystallography, Academic Press, New York, 1997, pp. 307–326.
[25] R.H. Blessing, Acta Crystallogr., Sect. A 51 (1995) 33.
[26] SMART and SAINT software for CCD diffractometers, version 6.1, Bruker AXS, Madison, WI, 2000.